Quarterly Progress Report

For Period

July 1 - September 30, 1966

FUNDAMENTAL STUDIES OF THE METALLURGICAL,
ELECTRICAL, AND OPTICAL PROPERTIES OF
GALLIUM PHOSPHIDE

Grant No. NsG-555

Prepared For

NATIONAL AERONAUTICS AND SPACE ADMINISTRATION
LEWIS RESEARCH CENTER
CLEVELAND, OHIO

Work Performed By

Solid-State Electronics Laboratories
Stanford University
Stanford, California

N67 10878
(ACCESSION NUMBER)

_____*33*_____
(PAGES)

CR-79722
(NASA CR OR TMX OR AD NUMBER)

FACILITY FORM 602

_____ (THRU)

_____/_____
(CODE)

_____*06*_____
(CATEGORY)

PROJECT 5109: ABSORPTION SPECTRA OF DIVALENT IRON IN II-VI
COMPOUNDS AND IN GaP

National Aeronautics and Space Administration
Grant NsG 555
Project Leader: G. L. Pearson
Staff: J. Baranowski

The research reported here is a continuation of our

systematic investigations of the transition group elements in GaP.

Transition metal impurities contain an incomplete d-shell whose

properties can be described in terms of crystal field theory. The

d-orbitals of the free atoms are well understood and in the weak

field scheme the effect of crystalline environment can be treated as

a perturbation. Observation of the optical absorption spectra due

to transitions within the d-shell will give the number of d-electrons

and the symmetry of their environment. The last quarter was mainly

devoted to studying the optical absorption spectra of iron in GaP.

The free iron ion has a $4s^2 3d^6$ configuration and the

ground state according to Hund's rule is ^5D. We can expect that iron

in GaP will produce the d^6 configuration if iron atoms substitute

for gallium atoms in the lattice and the Fermi level lies at or above

the iron acceptor level. The iron replacing gallium as an impurity

contributes two 4s electrons for bonding, leaving a d^6 configuration

and an unfilled acceptor level. The third electron needed for

bonding can be taken from free electrons in the conduction band

(filling the acceptor level) if the Fermi level is above the acceptor

level. Another possibility is that the third electron will be taken

from a d^6 configuration leaving a d^5 configuration. This can happen

if the Fermi level lies under the acceptor level.

The energy level scheme of a d^6 configuration in tetrahedral symmetry has been worked out theoretically by W. Low and M. Weger[1]. In this symmetry the ^5D level will split into an orbital doublet ^5E and an orbital triplet $^5T_2$. The spin-orbit coupling of first and second order will remove these degeneracies. This is presented in Fig. 1. The lowest level ^5E will be split only by second order spin-orbit splitting producing five discrete levels. Some of them will still degenerate so that according to the Jahn-Teller theorem[2], the impurity will displace itself to a lower symmetry to remove the degeneracy. This symmetry displacement will take place in the [100] direction. In our scheme presented in Fig. 1 this displacement is represented as an additional axial field in the [100] direction.

The energy levels of the ground state d^6 configuration are given in Table 1. Here Dq represents a constant factor and is a measure of the crystal field strength. A represents the axial contribution and λ is the spin-orbit coupling. To our knowledge the zero-phonon spectra of divalent iron in cubic fields has not yet been published. Accordingly, we have started our experimental work by looking at the spectra of iron in some II-VI compounds, where we can be sure that we are dealing with d^6 configurations. In addition, the solubility of iron in II-VI compounds is high so that it is easy to observe absorption spectra. The measurements were made at liquid helium temperature in a Perkin-Elmer 621 grating spectrometer. The spectra were taken from 4000 cm^{-1} to 2000 cm^{-1},

- 2 -

using a cryostat with sapphire windows. The sample was attached to the cold finger of the cryostat and its temperature was measured using a calibrated carbon resistor. It was about $8^{\circ}K$. Below we report the optical spectra of divalent iron in ZnSe, ZnTe, and CdTe.

a) Optical spectra of Fe^{+2} in ZnSe

For this work, single crystals of ZnSe doped with Fe were used which had been grown at SERL, Baldock, England. The optical spectrum is shown in Fig. 2; part of this spectrum taken with higher resolution is shown in Fig. 3.

The absorption spectrum consists of three main peaks connected with transitions from ground state to $^5T_2$ state which is split into three levels by first order spin-orbit splitting. The fine structure which appears on the low energy side of the spectrum is connected with transitions from the first four levels of the ground state ^5E, which are occupied according to a Boltzman distribution. We attribute these peaks to the following transitions (according to scheme in Fig. 1):

$$1 \rightarrow 8 = 2738 \text{ cm}^{-1}$$
$$2 \rightarrow 8 = 2722 \text{ cm}^{-1}$$
$$3 \rightarrow 8 = 2711 \text{ cm}^{-1}$$
$$4 \rightarrow 8 = 2693 \text{ cm}^{-1}$$

Because

$$1 \rightarrow 8 = 10 \text{ Dq} + 3\lambda + \frac{23}{5} \frac{\lambda^2}{Dq}$$

$$2 \rightarrow 8 = 10 \text{ Dq} + 3\lambda + \frac{20}{5} \frac{\lambda^2}{Dq}$$

We can calculate the exact value of the factor Dq and the spin-orbit coupling parameter λ. The results are

$$Dq = 293 \text{ cm}^{-1} \quad ; \quad \lambda = 188 \text{ cm}^{-1}$$

The value of spin-orbit coupling parameter λ is smaller than for the free divalent iron, which is 101 cm^{-1}(3). This small reduction may be caused by some screening of the electrostatic interaction between electrons within the d-shell.

The separation between the $2 \rightarrow 8$ peak and the $3 \rightarrow 8$ peak is only 11 cm^{-1} smaller than between the $1 \rightarrow 8$ and the $2 \rightarrow 8$ and between $3 \rightarrow 8$ and $4 \rightarrow 8$. This may be connected with existence of small Jahn Teller distortions A = 2.7 cm^{-1}.

Transitions to upper levels of the ${}^{5}T_{2}$ level are not so sharp. This broadening can be caused by interactions with different vibration modes. Without going into detail , we can say that the crystal field theory satisfactorily explains the optical spectra of iron in ZnSe.

b) Optical spectra of Fe^{+2} in ZnTe

Single crystals of ZnTe were prepared in the Department of Materials Science, Stanford University. Iron was evaporated on both surfaces of the sample and diffused at 1000°C for 24 hours. After that the sample was lapped and optically polished. The absorption spectrum of iron in ZnTe is shown in Fig. 4. The whole spectrum is compressed as compared with that for ZnSe. This comparison is caused by a reduction of the spin-orbit coupling parameter, to a value $\lambda \approx -50$ cm^{-1}. At the low energy side of the spectrum we have only

one strong peak at 2487 cm^{-1} with half width $\Delta\nu = 11$ cm^{-1} (see Fig. 5)

which is twice as broad as the 2738 cm^{-1} peak for ZnSe. Because of a

small value of spin-orbit coupling parameter λ, it is possible that

this peak consists of two peaks which cannot be resolved. The calcula-

ted second order spin-orbit splitting for this case is 5.7 cm^{-1},

comparable with thermal energy at $8^{\circ}K$. The next peak at 2472 cm^{-1}

can be connected with $5 \rightarrow 8$ transition if we have a pronounced Jahn

Teller distortion. A reduction in the spin-orbit coupling parameter

and the Racah parameters from free ion values would be expected in

the solid from ligand field theory, owing to the spread of the iron

d wave functions onto the neighboring ligands (Se or Te in the case

of Fe^{+2} in ZnSe or ZnTe). Another explanation of the reduction in

λ can be based on the dynamic Ham effect[4]. At this stage of the

work we are not able to say which of these two mechanisms is responsi-

ble for the reduction in spin-orbit splitting. It is possible that

both play important roles. The value of Dq obtained from the spectrum

is 263 cm^{-1}.

c) Optical spectra of Fe^{+2} in CdTe

In this study single crystals of CdTe were used which

had been prepared at Warsaw University, Poland. Iron was evaporated

on the surface of the sample and diffused at $960^{\circ}C$ for 24 hours. The

spectrum taken at liquid helium temperature is shown in Fig. 6. The

half width of the absorption band is the same as in ZnTe. The value

of the spin-orbit coupling parameter λ is -50 cm^{-1} and the value

of the crystal field parameter Dq is 238 cm^{-1}. The detailed structure

of the main peak is shown in Fig. 7. We interpret the peak at 2282 cm^{-1} as a transition $1 \rightarrow 8$ and $2 \rightarrow 8$ on the basis of the arguments given for ZnTe. The peak 2265 cm^{-1} is attributed to the transition $4 \rightarrow 8$. The origin of the two additional peaks at 2291 cm^{-1} and 2309 cm^{-1} is not well understood. In a corresponding region of the spectrum of ZnTe we see only a broad shoulder.

Conclusions

These preliminary results allow us to draw a few conclusions. The most important is that the spectra of divalent iron in II-VI compounds can be explained on the basis of low-field crystal field theory. The character of the spectra shows that iron occupies tetrahedral sites in the crystals studied. The measurements indicate that iron substitutes for zinc and cadmium in these materials. The zero phonon spectra allow us to give precise values of Dq, which is a measure of the crystal field strength and to see how this factor depends on lattice constant. This dependence is plotted in Fig. 8. Crystals with a higher lattice constant show a smaller value of Dq. The reduction of spin-orbit coupling parameter λ in tellurium compounds is also interesting. At this stage of the work, however, we have not enough experimental evidence to reach definitive conclusions on the behavior of λ.

Optical spectra of Fe^{+2} in GaP

Several diffusion runs of iron into polycrystalline GaP have been made. Iron was evaporated on both sides of the samples and diffused for 24 hours at temperatures ranging from $1270^{\circ}C$ to

1300°C. The samples were then lapped from both sides and optically polished. The absorption spectrum of divalent iron in GaP is shown in Fig. 9 for liquid nitrogen temperature , and in Fig. 10 for liquid helium temperature. The spectral range was extended to 4000 cm^{-1} by using a Cary 14 IR spectrometer. Part of the spectrum on the low energy side taken with five times higher resolution is shown in Fig. 11. This part of the spectrum is very similar to the corresponding one for ZnSe. As in the case of ZnSe we attribute the four peaks to the corresponding transitions:

$$1 \rightarrow 8 = 3349 \text{ cm}^{-1}$$
$$2 \rightarrow 8 = 3331 \text{ cm}^{-1}$$
$$3 \rightarrow 8 = 3321 \text{ cm}^{-1}$$
$$4,5 \rightarrow 8 = 3305 \text{ cm}^{-1}$$

The first two transitions allow us to calculate a parameter Dq and a spin-orbit coupling parameter λ. These give us:

$$Dq = 355 \text{ cm}^{-1}$$
$$\lambda = -87 \text{ cm}^{-1}$$

The position of the peak 3321 cm^{-1} is attributed to $3 \rightarrow 8$ transition and suggests a slight Jahn Teller distortion almost the same as in ZnSe - $A = 2.5$ cm^{-1}.

The next peak at 3305 cm^{-1} is attributed to transitions from the 4 and 5 levels to the 8 level. The separation between them is only 3 cm^{-1} if the Jahn Teller distortion is 2.5 cm^{-1}. The spectrum of iron which we have obtained indicates that we are dealing with a d^6 configuration in a tetrahedral coordination. This indicates that iron atoms replace gallium atoms substitutionally. The spectrum of

divalent iron in gallium phosphide can therefore be explained on
the basis of crystal field theory, and equally as well as in ZnSe
(which is a much more ionic crystal). The value of $Dq = 355 \text{ cm}^{-1}$,
which is higher than for II-VI compounds, shows a higher degree of
covalency[7].

It may appear surprising that crystal field theory,
originally developed for ionic environments, works well for a co-
valent system such as iron-doped gallium phosphide. This indicates
that the bonding and d-orbitals do not interact strongly as has
usually been assumed. The results of previous work in our laboratory[6]
on GaP doped with cobalt, and the results reported here, show that
crystal field theory can be used to obtain detailed electron models
of semiconductor impurities. These are the first experimental
indications that this approach to deep-lying impurity levels in
semiconductors is a valid one.

The absorption spectra presented in Figs. 9, 10 and 11 are
the result of a 24-hour diffusion of iron at 1280°C. It is very
difficult to get spectra of divalent iron in GaP. Several samples
showed no structure at all in this region except for a steadily increas-
ing absorption with wavelength, typical for p-type GaP. The Fermi
level was below the acceptor level of iron and we were probably
dealing therefore with a d^5 configuration. This change of type
could be caused by a diffusion of copper from quartz (the solubility
of a copper in GaP is high), producing shallow acceptor levels.

Those samples which were strongly n-type showed a strong
absorption between 4000 cm^{-1} and 3000 cm^{-1}. This absorption is

- 8 -

without any structure at liquid helium temperature and is caused by transitions between conduction bands[8].

In the next quarter we shall continue a study of iron in GaP. We are interested also in a study of GaP doped with cobalt and zinc. This system also should produce a d^6 configuration with one d-electron in a bonding orbital. We have made some preliminary measurements of photoconductivity in p-type GaP doped with Co and Zn. This will be reported in the next quarter.

REFERENCES

1. W. Low and M. Weger, Phys. Rev., 118, 1119 (1960).

2. H. A. Jahn and E. Teller, Proc. Roy. Soc. (London) A161, 220 (1937).

3. D. S. McClure, Solid Stae Physics, 9, Academic Press Inc. 1959

4. F. S. Ham, Phys. Rev., 138, A1727 (1965).

5. R. Pappalardo and R. E. Dietz, Phys. Rev., 123, 1182 (1961).

6. D. H. Loescher, J. W. Allen, G. L. Pearson, Paper presented at the International Conference on the Physics of Semiconductors, Kyoto, September 1966.

7. A. D. Liehr, C. T. Ballhausen, Jour. Mol. Spectroscopy 2, 342 (1958); 4, 190 (E) (1960).

8. J. W. Allen and J. W. Hodby, Proc. Phys. Soc., 82, 315 (1963).

FIGURES

Fig. 1   Energy level scheme of ^5D in combined tetrahedral and axial fields. The figure shows the levels as split by the field and by spin-orbit coupling. The energy of the levels is given in Table I according to the numbers next to the level.

Fig. 2   Absorption spectrum of ZnSe: Fe at liquid helium temperature.

Fig. 3   ZnSe: Fe expanded absorption in the 2700 cm^{-1} region.

Fig. 4   Absorption spectrum of ZnTe: Fe at liquid helium temperature.

Fig. 5   ZnTe: Fe expanded absorption in the 2500 cm^{-1} region.

Fig. 6   Absorption spectrum of CdTe: Fe at liquid helium temperature.

Fig. 7   CdTe: Fe expanded absorption in the 2300 cm^{-1} region.

Fig. 8   Effect of lattice constant on magnitude of Dq in II-VI
          compounds. The value of Dq for CdS was calaculated from
          the results of R. Pappalardo and R.E. Dietz[5] taken at
          liquid nitrogen temperature.

Fig. 9   Absorption spectrum of GaP: Fe at liquid nitrogen
          temperature.

Fig. 10   Absorption spectrum of GaP: Fe at liquid helium temperature.

Fig. 11   GaP: Fe expanded absorption in the 3300 cm^{-1} region at
          liquid helium temperature.

TABLE 1   - Energy levels of the ground state of the d^6 configuration in a tetrahedral field and axial field in the (100) direction. The axial field is of the same order as the second order spin-orbit coupling $(Dq \gg \lambda;\ \lambda^2/Dq \approx A;\ A > 0)$

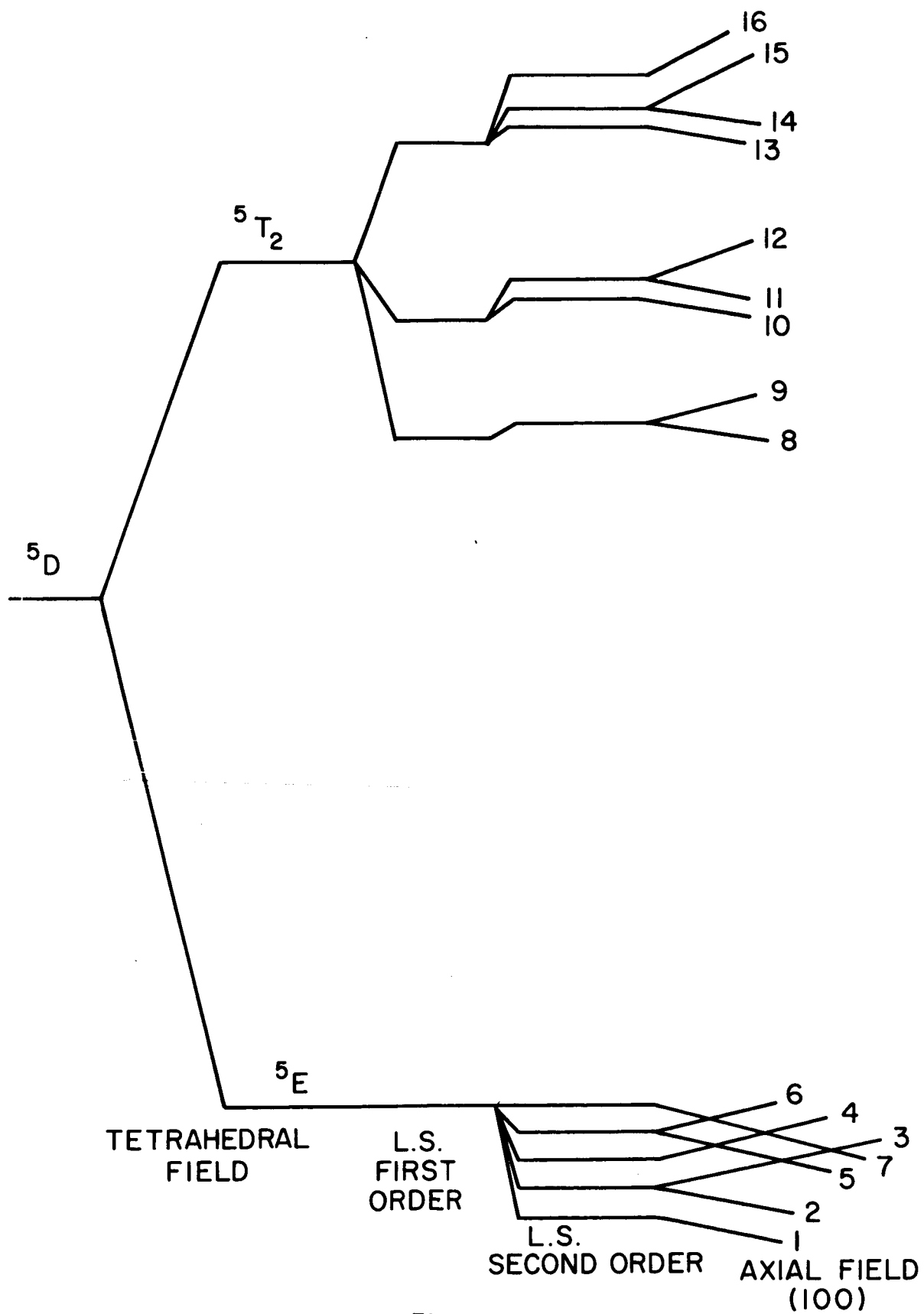| Energy Levels	Total Degeneracy
$E_1 = -6Dq - 4\frac{3}{5}\frac{\lambda^2}{Dq} - 2A$	1
$E_2 = -6Dq - 3\frac{3}{5}\frac{\lambda^2}{Dq} - 2A$	2
$E_3 = -6Dq - 3\frac{2}{5}\frac{\lambda^2}{Dq} + 2A$	1
$E_4 = -6Dq - 2\frac{3}{5}\frac{\lambda^2}{Dq} + 2A$	2
$E_5 = -6Dq - \frac{3}{5}\frac{\lambda^2}{Dq} - 2A$	1
$E_6 = -6Dq - \frac{3}{5}\frac{\lambda^2}{Dq} + 2A$	2
$E_7 = -6Dq - 2A$	1
$E_8 = 4Dq + 3\lambda + \frac{9}{25}\frac{\lambda^2}{Dq} - A$	2
$E_9 = 4Dq + 3\lambda + \frac{9}{25}\frac{\lambda^2}{Dq} + 2A$	1
$E_{10} = 4Dq + \lambda + \frac{3}{5}\frac{\lambda^2}{Dq} - A$	3
$E_{11} = 4Dq + \lambda + 2\frac{3}{5}\frac{\lambda^2}{Dq} - A$	1
$E_{12} = 4Dq + \lambda + 2\frac{3}{5}\frac{\lambda^2}{Dq} + 2A$	1
$E_{13} = 4Dq - 2\lambda + \frac{2}{5}\frac{3}{5}\frac{\lambda^2}{Dq} - A$	3
$E_{14} = 4Dq - 2\lambda + 2\frac{3}{5}\frac{\lambda^2}{Dq} - A$	1
$E_{15} = 4Dq - 2\lambda + 2\frac{3}{5}\frac{\lambda^2}{Dq} + 2A$	2
$E_{16} = 4Dq - 2\lambda + 4\frac{3}{5}\frac{\lambda^2}{Dq} + 2A$	1

$^5T_2$

^5D

^5E

16
15
14
13

12
11
10

9
8

6
4
3
7
5
2
1

TETRAHEDRAL
FIELD

L.S.
FIRST
ORDER

L.S.
SECOND ORDER

AXIAL FIELD
(100)

Fig.1

Zn Se + Fe
THICKNESS 0.76 mm
LIQUID HELIUM TEMP

2600 cm⁻¹   3000   3500   3900 cm⁻¹

Fig.2

Fig.3

ZnTe + Fe
LIQUID HELIUM TEMP
THICKNESS 100 μ

ABSORPTION

2500   3000 cm⁻¹

Fig.4

2487

ZnTe + Fe

Slits

$\Delta \nu = 11\ \mathrm{cm}^{-1}$
(HALF WIDTH)

2472

ABSORPTION

2450   2490   cm⁻¹

Fig. 5

CdFe + Fe
LIQUID HELIUM TEMP
THICKNESS 250 μ
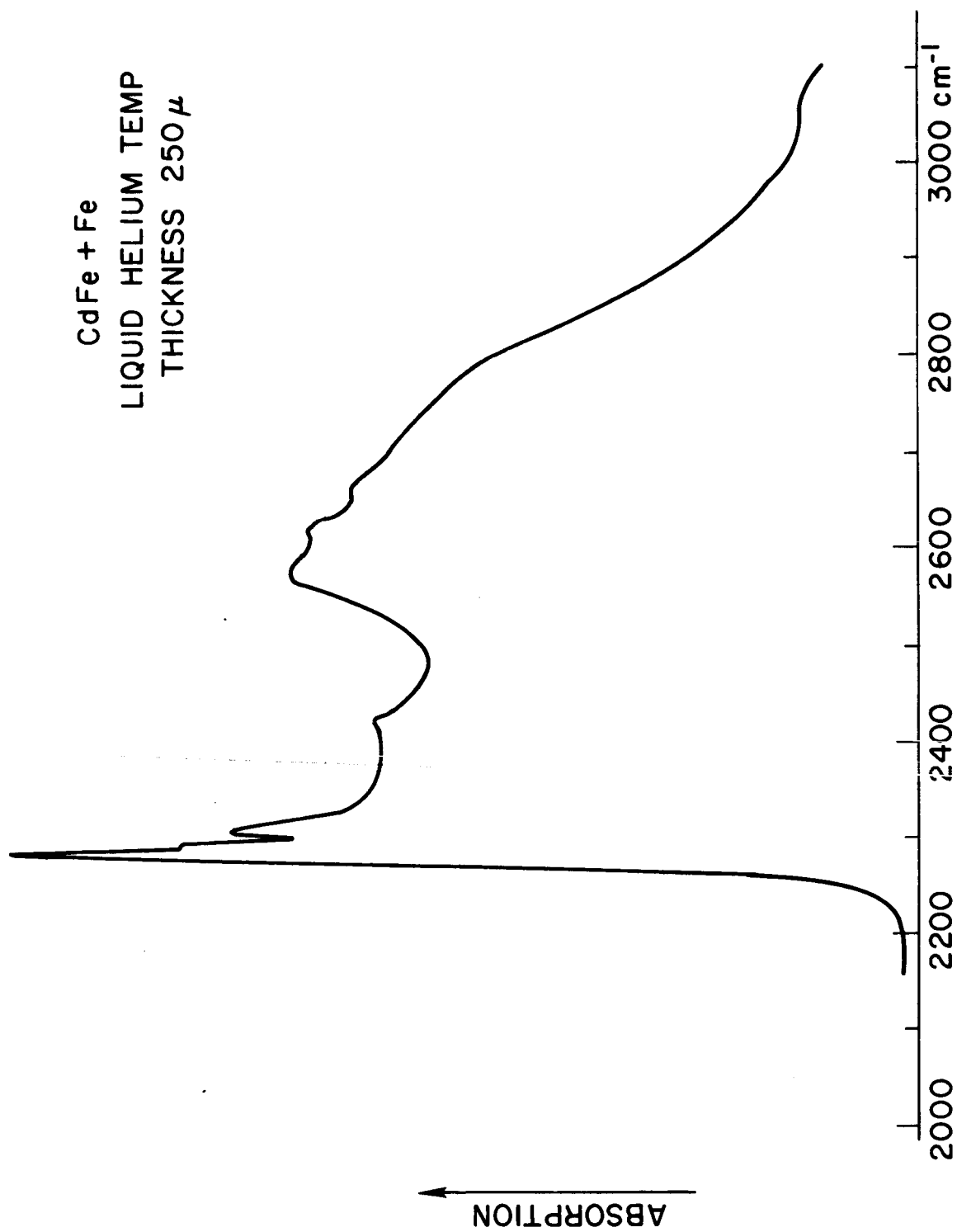
ABSORPTION

2000   2200   2400   2600   2800   3000 cm⁻¹
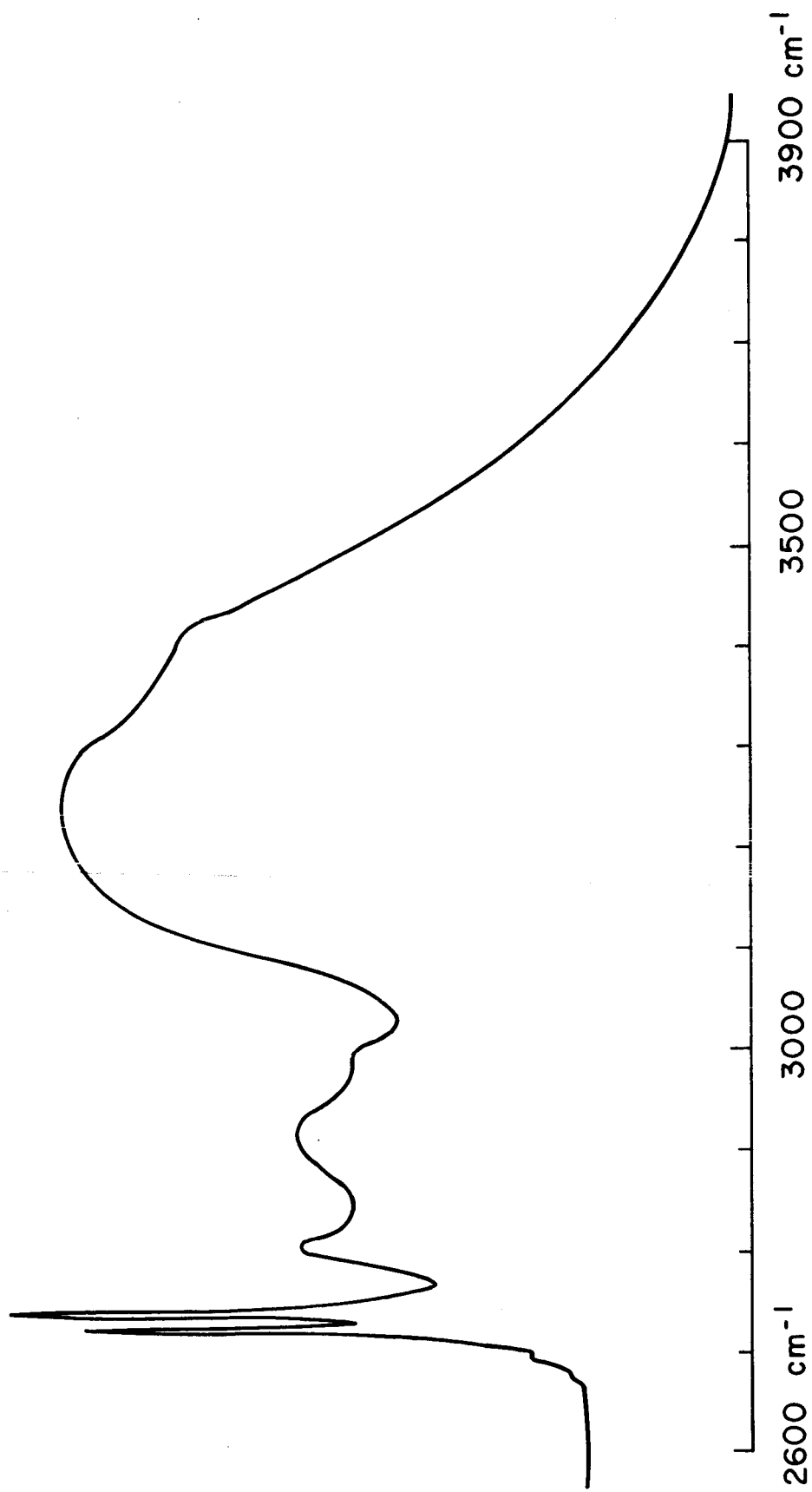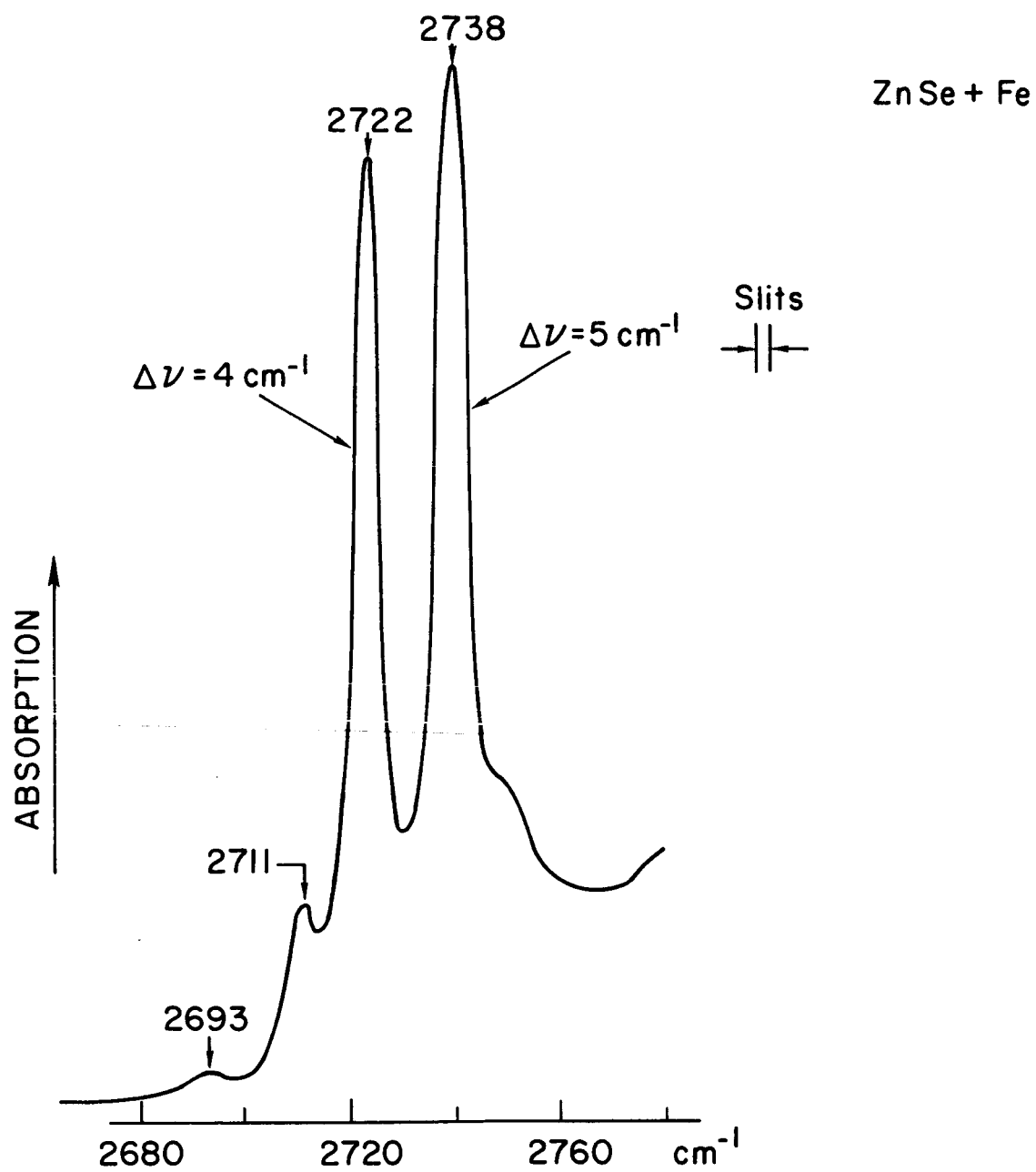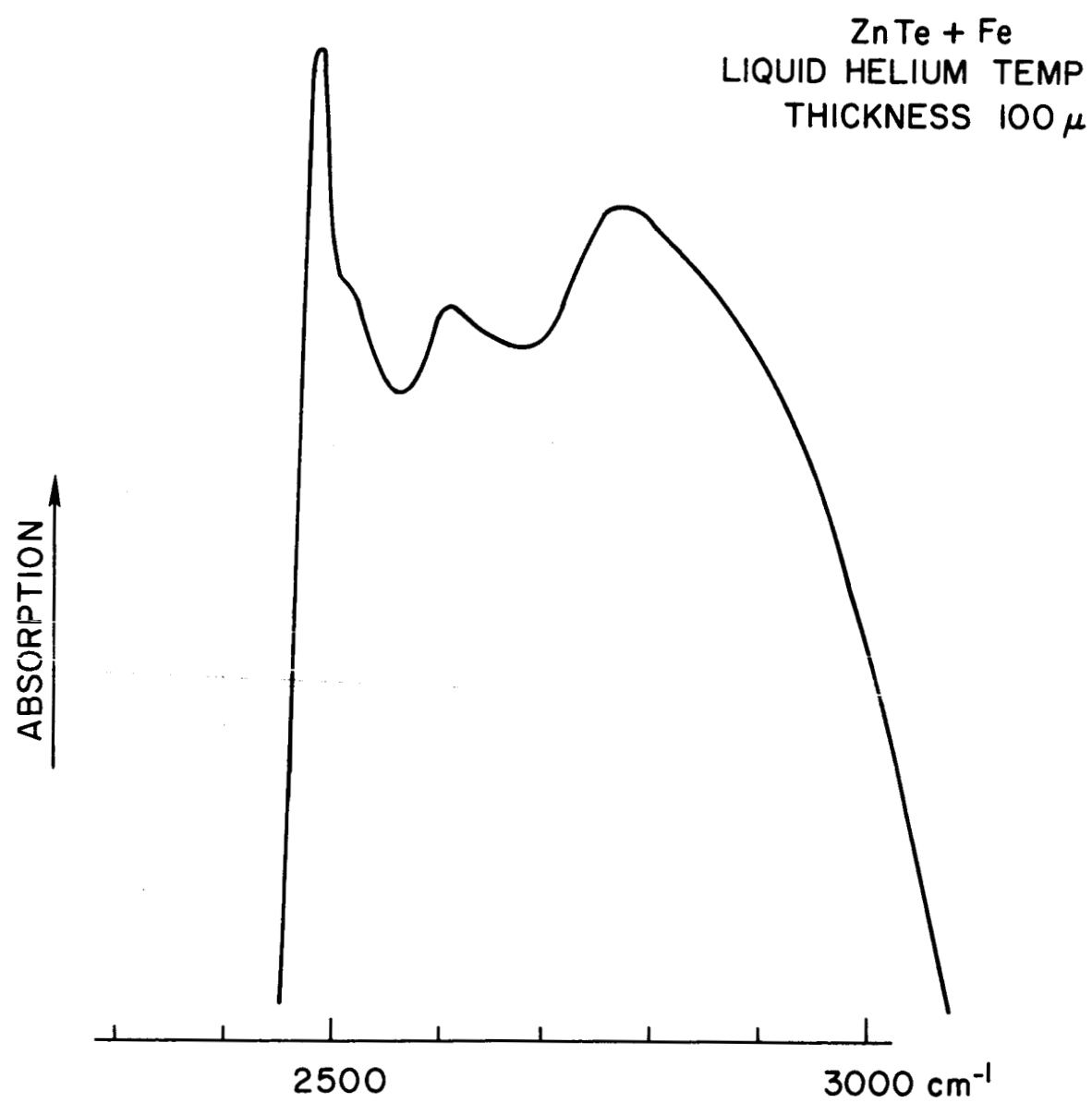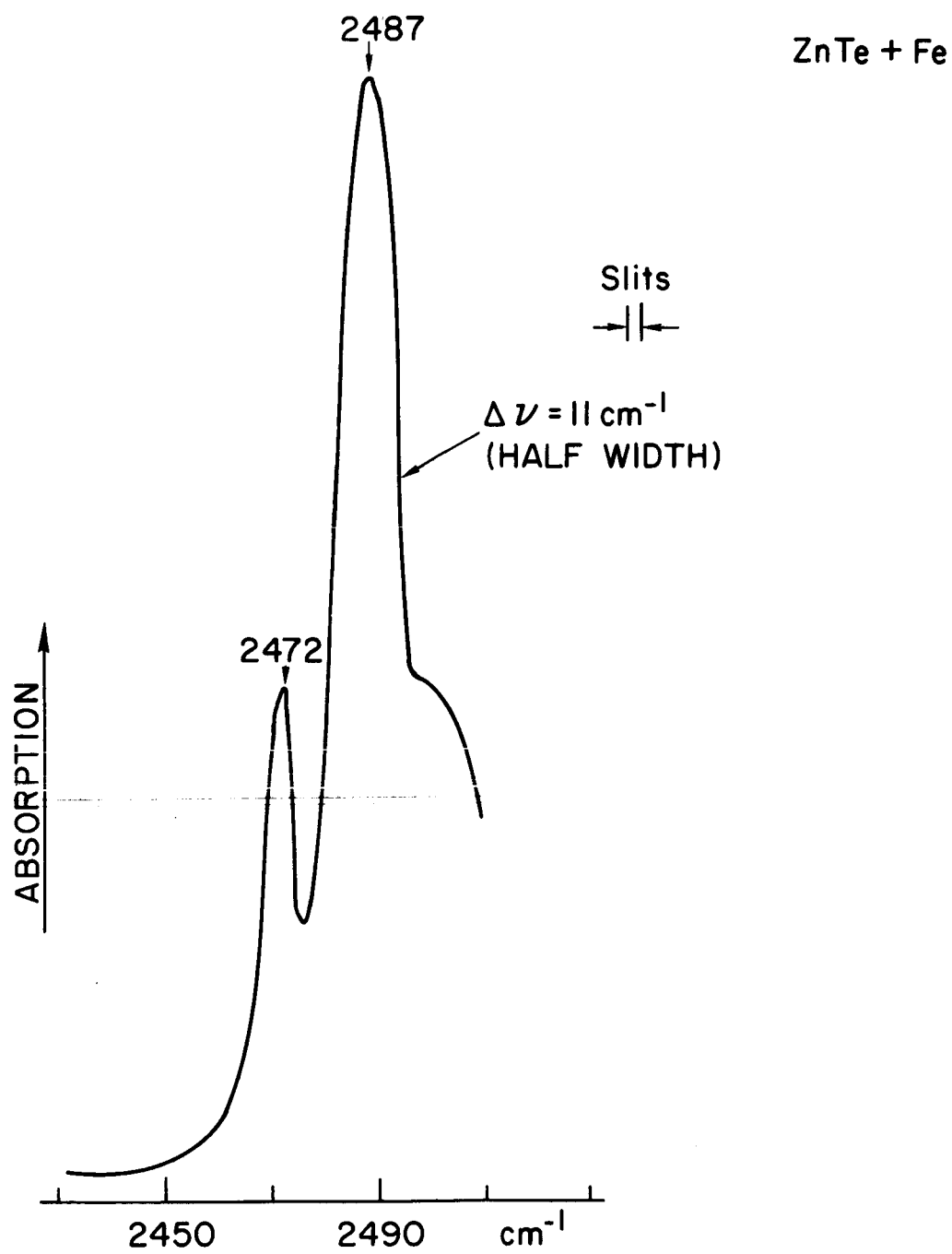
Fig.6
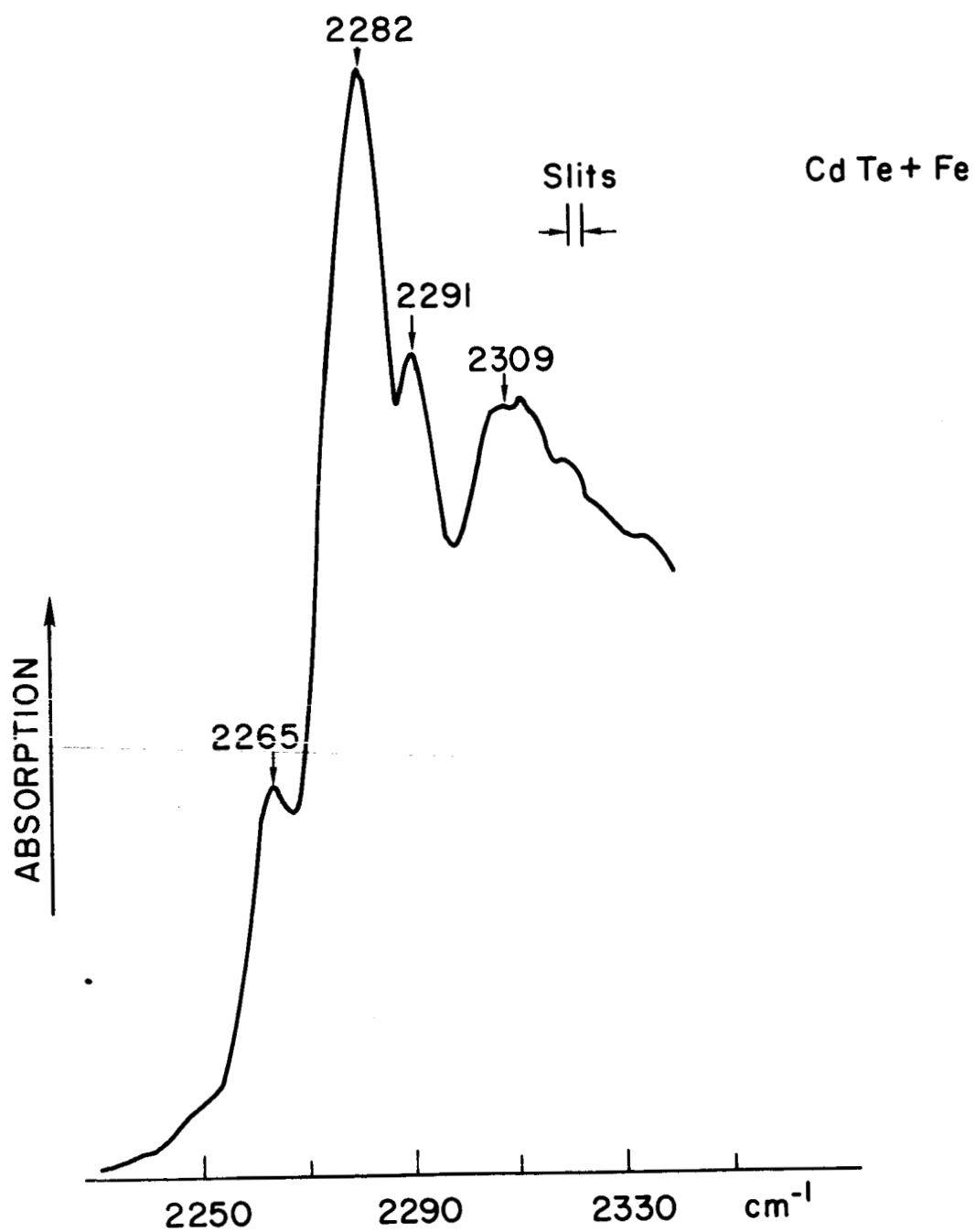
Fig. 7
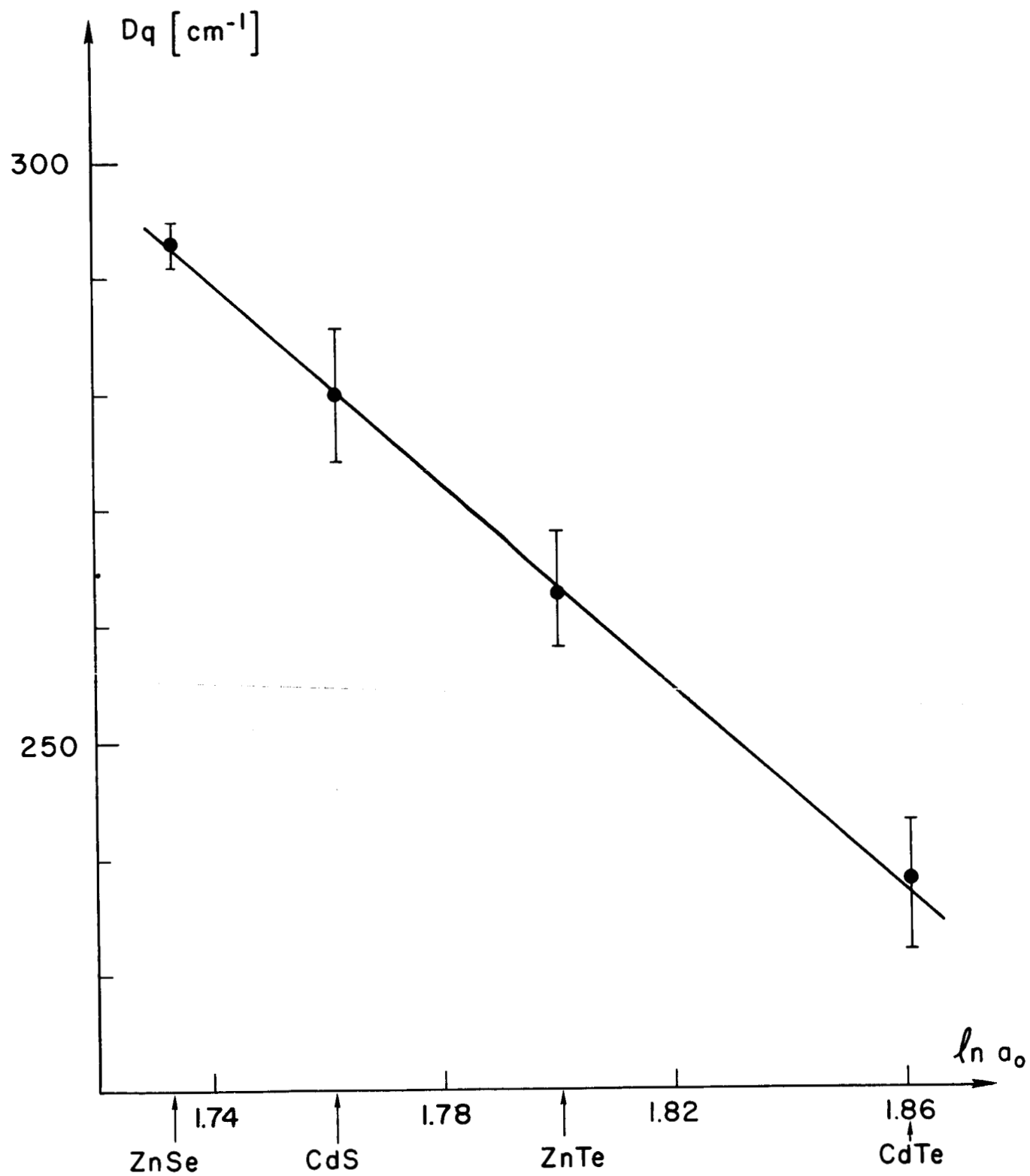
Fig.8

GaP + Fe (SAMPLE 2)
LIQUID NITROGEN TEMP
THICKNESS 1.2 mm

ABSORPTION
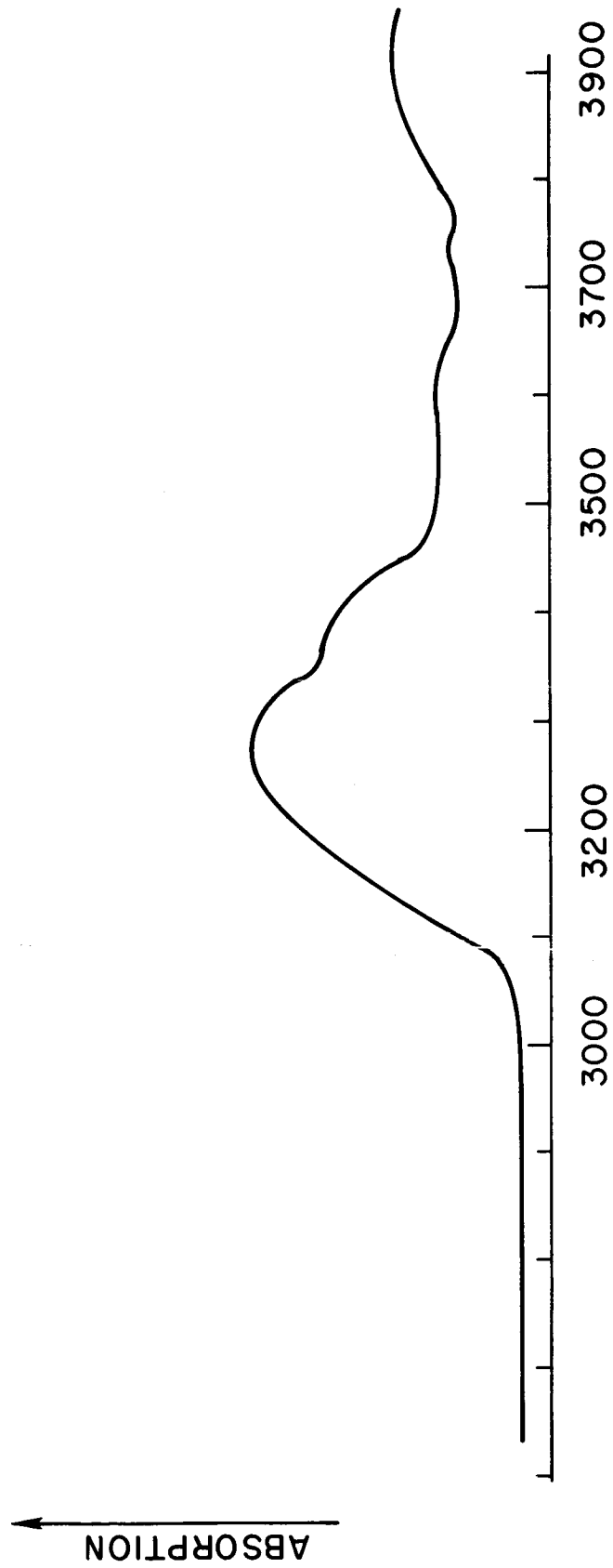
3000 3200 3500 3700 3900

Fig.9

GaP+Fe (SAMPLE 2)
LIQUID HELIUM TEMP
THICKNESS 1.2 mm

ABSORPTION

3349

3331

3321

3305

3410

3630

3200   3400   3600   3800   4000   4200   4400 cm⁻¹
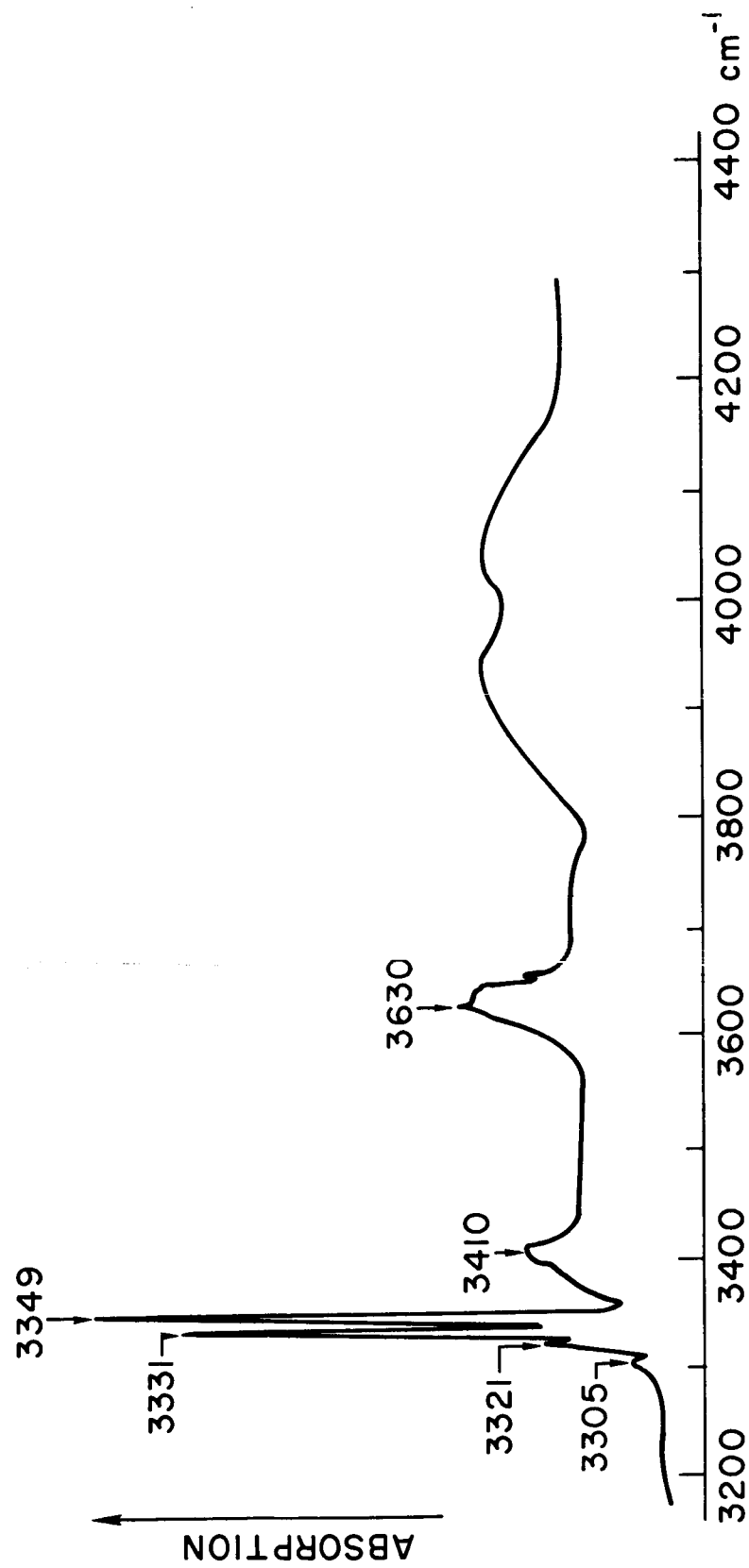
Fig.10

GaP + Fe (SAMPLE 2)

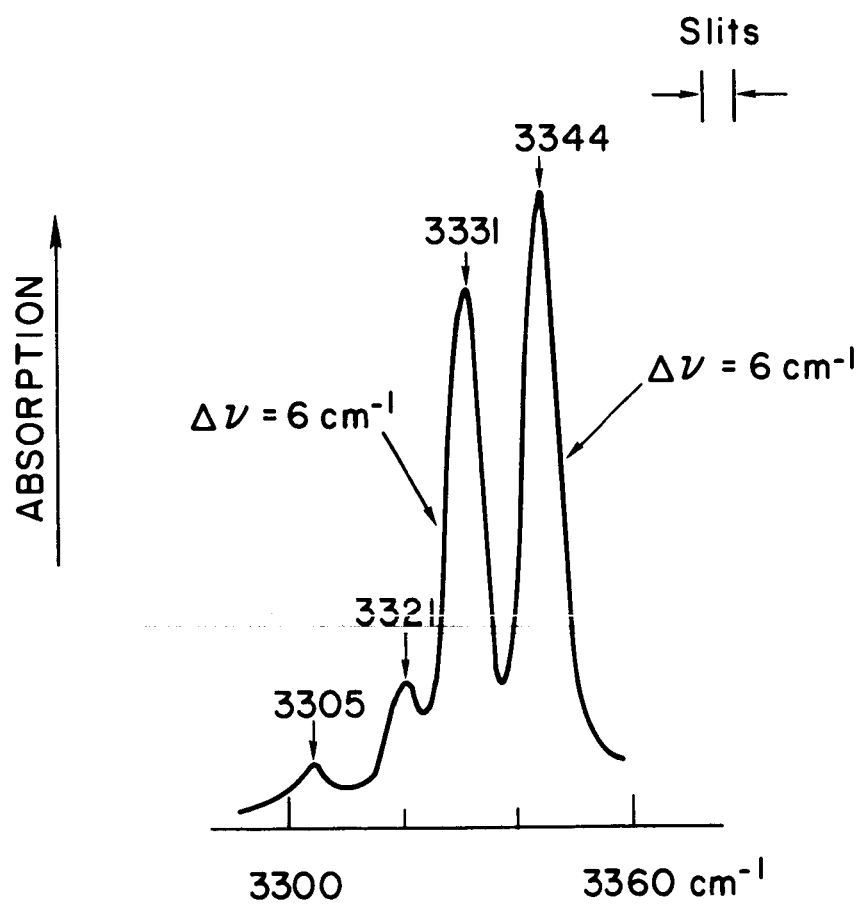Fig. 11

PROJECT 5112: THE PROPERTIES OF RECTIFYING JUNCTIONS IN $GaAs_xP_{1-x}$

National Aeronautics and Space Administration
Grant NsG-555
Project Leader: G. L. Pearson
Staff: S. F. Nygren*

The purpose of this project is to study the preparation
and characterization of rectifying junctions in GaP and $GaAs_xP_{1-x}$.
In particular, we wish to relate the structure of the crystals to
the electrical properties of the junctions.

A. Imperfections in Gallium Phosphide Crystals

Work done under this project in previous quarters has
revealed that all of the GaP crystals grown epitaxially in this
laboratory contain planar imperfections that are parallel to {111}
planes. When zinc from an elemental source is diffused into a
GaP crystal with these imperfections, it apparently diffuses down
the imperfections more quickly than it diffuses through the bulk.
This leads to a diffusion front that is not planar; it contains
many spikes. Since zinc is the impurity most commonly used as an
acceptor in GaP, it is worthwhile for us to determine the nature of
the planar crystal imperfections and the mechanism by which these
diffusion spikes are formed.

During this quarter our investigations have been con-
cerned with characterizing the planar crystal imperfections. Be-
cause these imperfections are parallel to {111} planes, which are
close-packed, we suspect that the imperfections are either stacking

---

faults or slip traces. A stacking fault is the imperfection that occurs where the {111} planes of the crystal are not stacked in the usual order. Such an imperfection does not, by itself, involve any dislocations or place any strain on the crystal. If a stacking fault does not extend all the way to the edge of the crystal, however, it must end in a partial dislocation. A slip trace results when two {111} planes slide across each other. This leaves a set of parallel dislocations between the planes that slipped.

B. Etching

Typically, a dislocation etchant reveals the planar imperfections in the crystals as straight grooves etched into the crystal surface at the intersections of the imperfections and the surface. If a light etch were to reveal that an etch groove is really a set of etch pits which are very close together, we would have strong evidence that the pits correspond to dislocations and that the set of dislocations mark a slip trace. If a light etch revealed that grooves have smooth bottoms, then we might be observing either a stacking fault or a slip trace in which the dislocations are so close together that they cannot be resolved.

We etched two GaP samples lightly (3 to 5 minutes at room temperature) in 8 $K_3Fe(CN)_6$: 12 KOH: 100 H_2O. The resulting groove bottoms were not smooth, but under 1000 times magnification it was not possible to tell if the unevenness in the bottoms of the grooves was facets or rows of etch pits. It was observed that some etch grooves end in a row of pits. However, continuing to etch

the sample for an extended period of time did not make the pits merge into a groove.

C. Birefringence

If a perfect, unstrained crystal of a transparent cubic material were observed in transmitted light in a polarizing microscope, no light should be transmitted when the polarizers are crossed. If such a crystal is strained, however, a plane-polarized light wave entering the sample is split into two components which are plane polarized in the directions of the principle stresses [Ref. 1]. Thus, if the crossed polarizers are rotated into a position where the direction of a principle stress in the crystal is the same as the direction of polarization of the polarizer, the crystal will not affect the polarization of the light, and no light will be transmitted. If the crossed polarizers are rotated into any other position, light will be transmitted. Hence, the orientation of strain in a crystal may easily be found by placing the crystal in a polarizing microscope. One finds a spot in the crystal where light is transmitted. Then one rotates the crossed polarizers until the light is extinguished; the polarizer is then oriented in the same direction as a principle direction of stress.

Since GaP is cubic and is transparent to all visible light with a wavelength longer than about 5600 $\overset{o}{A}$, birefringence may be used to learn much about strain in GaP. Preliminary experiments suggest that the directions of the principle stresses are parallel to and perpendicular to the etch grooves. However,

the stress field does not appear to be homogeneous along the length of an etch groove. Light may be transmitted through the crystal by birefringence only along a small fraction of the length of a groove; no light may be transmitted along the rest of the groove no matter what position the crossed polarizers are rotated into.

D. Lang Topography

In the Lang method of x-ray topography, a collimated beam of x-rays is transmitted through a crystal in such a way that part of it is refracted through a Bragg angle. The transmitted beam is blocked, and the refracted beam is allowed to make an image on photographic film. The crystal and the film are simultaneously moved in such a way that the entire crystal is scanned by the x-ray beam. If the crystal is perfect, the film will be uniformly exposed in the region that corresponds to the crystal. If there is any strain in the crystal, or if there are any imperfections in the crystal that have associated strain fields (e.g., dislocations), these strain fields will be mapped onto the film since the strain disturbs the Bragg refraction. This technique has been used quite successfully to make a photographic record of the locations and interactions of dislocations in crystals [Ref. 2].

We have attempted to make Lang topographs of our GaP crystals, but our attempts have been unsuccessful. We take this lack of success as further evidence for two things:

1. The crystals contain a high concentration of dislocations. We typically observe dislocation densities of

3×10^5 cm^{-2}, and we have observed clusters as high as 3×10^7 cm^{-2}.

Lang [Ref. 2] gives 1×10^6 cm^{-2} as the limit of resolution for topographs in silicon.

2. The crystals are very highly strained. Since imperfections are revealed in Lang topographs because of their strain fields, additional strain will mask the imperfections. There are two additional experimental results that suggest a large amount of strain. First, a large amount of light is transmitted through our GaP crystals when they are observed under crossed polarizers. Second, Allen [Ref. 3] has reported that our GaP crystals spontaneously cleave into small pieces when they are lapped thinner than two or three thousands of an inch.

REFERENCES

1. A. W. Hendry, Photoelastic Analysis, Pergamon Press, 1966.
2. A. R. Lang, J. Appl. Phys., 30, 1748 (1959).
3. J. W. Allen, private communication.

PROJECT 5116:   DONOR IMPURITIES IN GaP

The purpose of this project is to study the

behavior of shallow donors in gallium phosphide. In particular S,

Se, and Te will be diffused into GaP to determine solubilities and

diffusion parameters. This information will be useful in delineating

the properties of GaP doped with these shallow donor impurities.

A. Crystal Growth

During the last quarter, 14 undoped GaP single

crystals were grown by the open tube method developed by Chen and

Loescher in this laboratory. Measurements of the electrical proper-

ties of some of these crystals are shown in Table 1, along with the

three crystals reported previously. The cause of the poor crystals,

which generally occur at the beginning of a series of growths, is

not known. Work is underway to determine and eliminate this

unknown factor in the growth conditions.

B. Diffusion Considerations

Since there has been no report on the diffusion of

sulfur into GaP, it is necessary to guess at the diffusion coefficient

of S in GaP in order to estimate the required diffusion time. We

can extrapolate from reports of sulfur diffusion into GaAs by using

---

*NSF Fellow

the following empirical formula:

$$D_{T_1}(GaAs) = D_{T_2}(GaP) \quad \text{where}$$

$$\frac{T_1}{T_2} = \frac{T_m(GaAs)}{T_m(GaP)} = m$$

that is, the diffusion coefficient of sulfur in GaAs at temperature

T_1 is the same as that of sulfur in GaP at T_2 where T_1/T_2 is equal

to the ratio of the melting temperature of the two materials. This

is equivalent to the statement that if

$$D\ (GaAs) = D_o \exp - Q/kt \quad \text{then}$$

$$D\ (GaP) \ = D_o \exp - Q/mkt$$

The empirical formula does not always give very satisfactory results.

However, it is useful as a first approximation in the absence of

any other information.

Using Kendall's data[1] for sulfur in GaAs, we find

that the diffusion coefficient for S in GaP is 6 x 10 cm^2/per sec.

at 1200°C, about an order of magnitude less than in GaAs. Thus for

a penetrator depth of 1 mil, diffusion times approximately 24 hours

long will be required.

C. Practice Diffusion (experimental)

In order to perfect experimental techniques, a

number of 24 hour diffusions have been carried out at 1200°C. In

this we place sulfur (non-radioactive), phosphorus and the undoped

GaP sample into an ampoule, evacuate to 10^{-5} torr, and seal. Since

we are working within the solidus region in a ternary system, it

is necessary to s pecify two parameters in addition to the temperature

in order to completely specify the system. A convenient choice of variables is the pressures of the sulfur and phosphorus in the ampoule during diffusion. Consideration of the ternary phase system Ga-P-S and experimental limitations have led to the use of phosphorus (P_2) pressures between 2×10^{-2} and 1 ATM and sulfur pressures between 10^{-3} ATM and 1 ATM - on the one hand, pressures cannot be so high as to cause explosions while on the other hand, sufficient amounts of sulfur must be present so that the amount diffused into the sample is small compared to that in the surrounding vapor. Control samples with no sulfur source were also placed in the furnace.

As a result of these diffusion experiments, it has been found that serious surface attack to the GaP samples occurs. It is believed that vapor transport of the GaP sample occurs - similar to the reaction used in closed tube epitaxial growth of GaP - where GaP from the sample is carried by some transport agent, presumably water molecules or sulfur atoms and deposited at some cooler spot on the walls of the ampoule.

The equivalent surface loss is generally 2 - 3 microns when no sulfur is present and approximately 8 - 10 microns with sulfur present. Since the removal of the GaP from the surface is not uniform, the actual surface roughness is greater than this. Since sulfur is expected to diffuse in only 25 microns for a 24-hour diffusion at $1200^{O}C$, this surface loss will cause large errors in the data.

Some modifications of experimental technique are being considered which will hopefully overcome the transport difficulty. We are also planning several experiments with selenium next quarter to see whether similar difficulties arise in the Ga-P-Se system.

REFERENCES

1. D. L. Kendall, Stanford Report SU-DMS 65-29, p.48, August 1965.

TABLE 1 - Resistivity and Mobility of Undoped GaP Single Crystals
Grown During this Quarter

Crystal No.	Resistivity (ohm-cm)	Hall Mobility (cm^2/v-sec)	Carrier Concen. (cm-3)
1	23.6	96	2.8×10^{15}
2	7.9	112	7×10^{15}
3	24.8	60	5×10^{15}
4	51	59	2.1×10^{15}
5	45.5	86	1.6×10^{15}
6	No Measurement -	good crystal	
7	14.8	105	4×10^{15}
8	406	27	5.7×10^{14}
9	No Measurement -	poor crystal	
10	No Measurement -	poor crystal	
11	"	good	
12	"	"	
13	"	"	
14	"	poor crystal	
15	"	good crystal	
16	"	"	
17	"	"	